Research Center Space
Universität der Bundeswehr München

Session C3: Signals of Opportunity-Based Navigation Systems 1

LTE transmitter states estimation using a combined code and carrier phase observation model

Muhammad S. Hameed, Markel Arizabaleta-Diez, Mathias Philips-Blum and Thomas Pany

Universität der Bundeswehr München

Overview - State of the Art with LTE/5G Positioning

LTE Positioning

Network based
- Standardized in LTE Release 9 with Positioning Reference Signal (PRS) [1]
- Dedicated resource allocation [2][3]:
  - Requires additional bandwidth => constraint on provider
  - Cellular provider specific => not transmitted by all providers
  - User position shared with network => privacy compromised

UE Based
- Based on TOA estimation using synchronization dedicated signal resources e.g PSS, SSS and CRS.
- TOA estimation (advanced signal processing) techniques [4]:
  - First peak detection technique
  - Statistical modeling of CIR
  - Super-resolution algorithm
  - Delay-lock loop
- SOTA LTE receiver [3][5]:
  1. Acquisition and tracking of LTE using PSS and SSS
  2. Obtain first estimate of TOA using SSS
  3. Update of TOA estimate based on CIR estimated using CRS

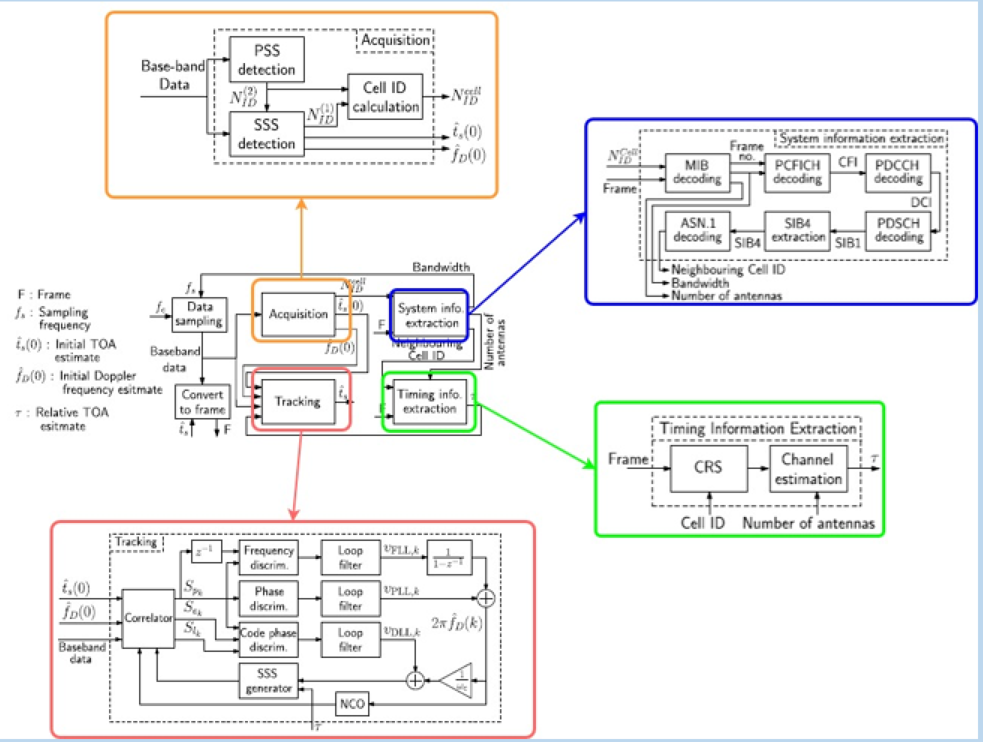

State-of-the-art LTE receiver for positioning [3]

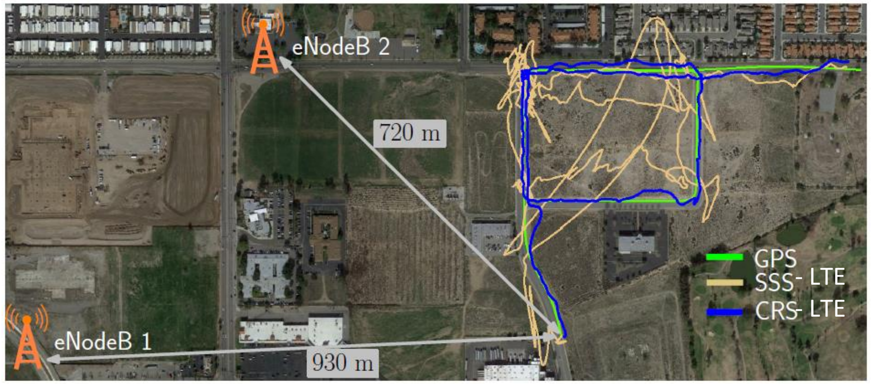

Vehicle-mounted receiver's GPS trajectory and trajectories estimated with LTE SSS and CRS signals [5]

5G Positioning

Indoor Positioning
- Extension of TOA estimation for indoor environments.
- Mixed Line-Of-Sight (LOS) / Non-Line-Of-Sight (NLOS) environment.
- Reducing NLOS errors through [6]:
  - Smart selection of base station [7]
  - Virtual base station mapping for NLOS signals [8]
  - NLOS propagation model compensation [9]

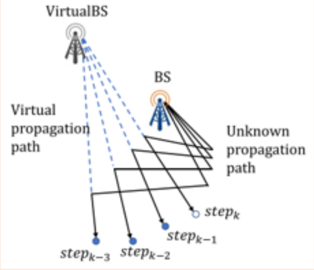

Virtual base station concept [6]

Urban canyon to indoor positioning evolution

LTE signal introduction and MuSNAT implementation

- **LTE tracking approach** -> generation of a single time-domain replica of the LTE SSS or CRS signal and using conventional GNSS-like DLL,PLL and FLL tracking.
- Code tracking achieved by cross-correlating measured signal with SSS/CRS code replica for complete LTE frame length (= 10 ms)

Each ‘vertical’ thin line represents an OFDM symbol of duration 66.6 us.

LTE frame within a measured signal transmitted from Amarisoft BS

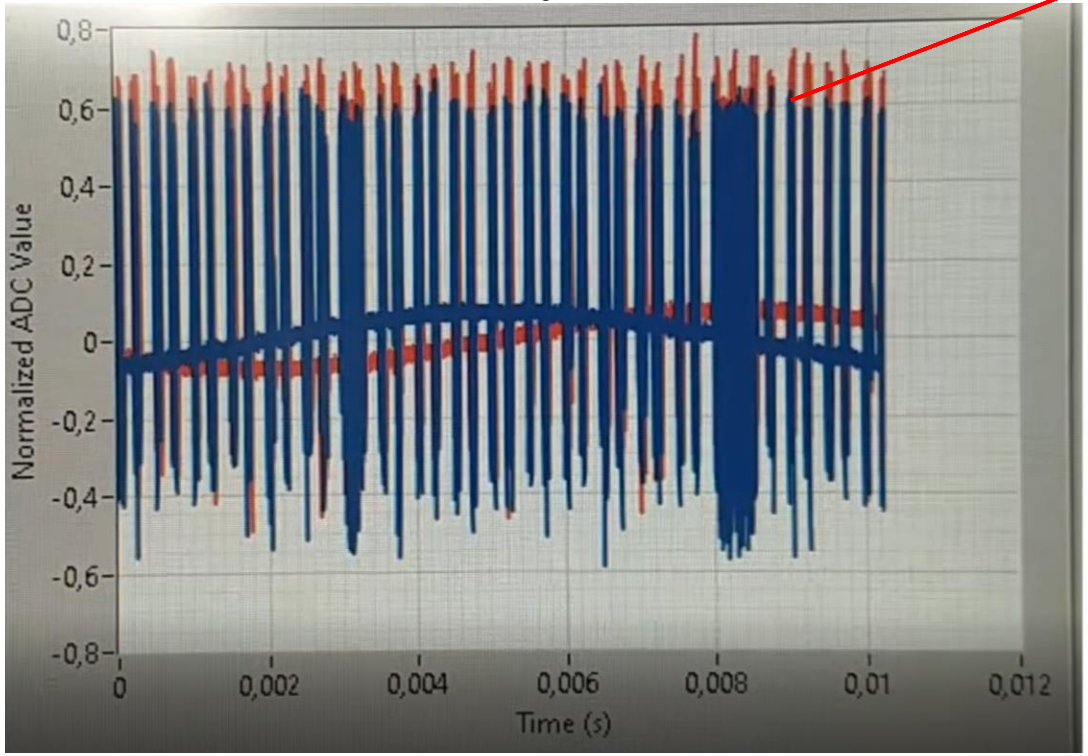

Time series of LTE CRS signal code replica for 10 subframes and 50 RBs

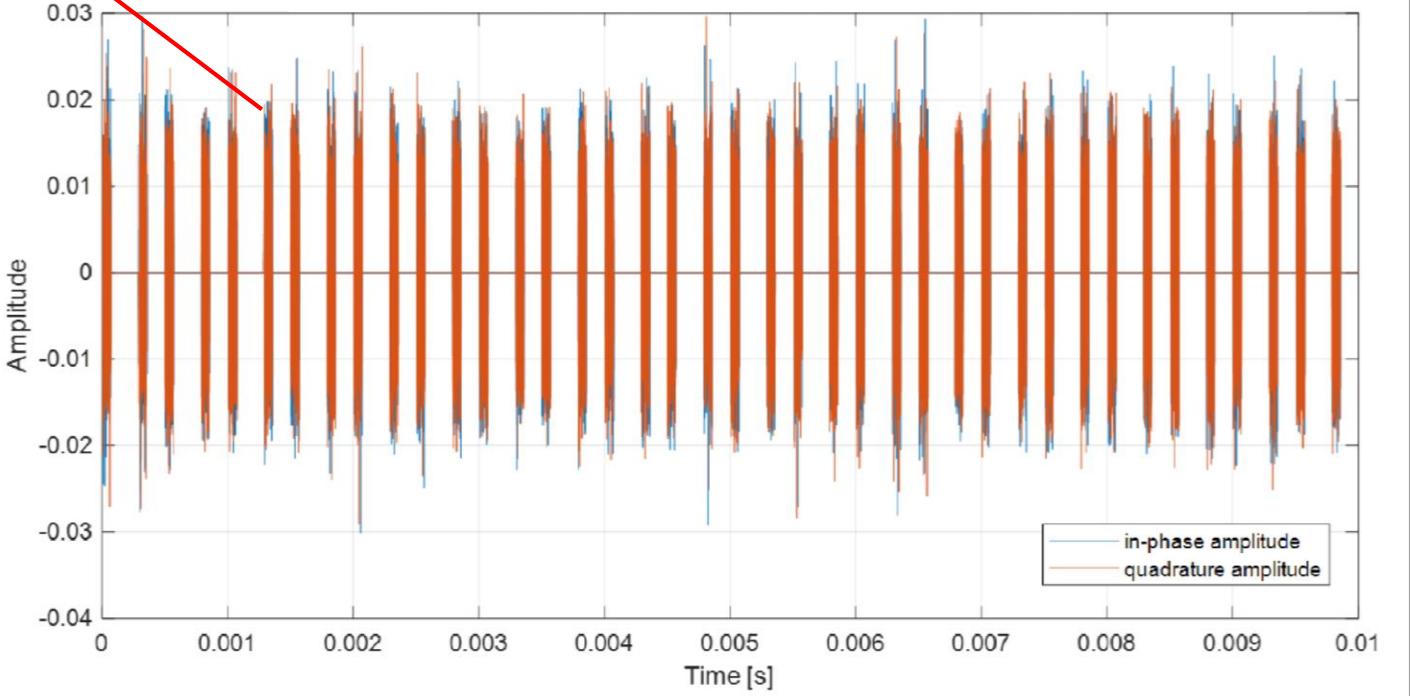

SSS vs CRS signal comparison

SSS

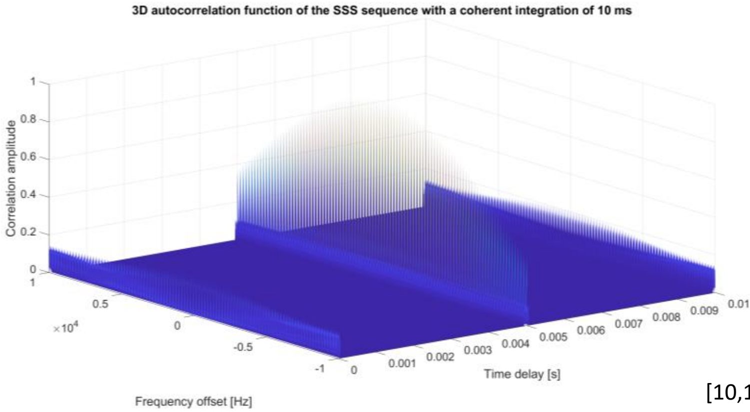

[10,11]

Transition from SSS based tracking to CRS based tracking

Pros:

- Higher bandwidth → narrower correlation peak → low tracking jitter
- Less Doppler side-peaks

Cons:

- More secondary peaks in code phase domain → solvable using **BumpJump**

CRS

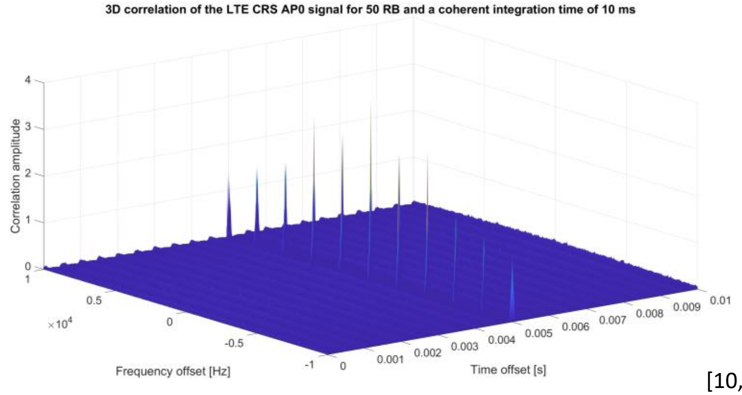

[10,11]

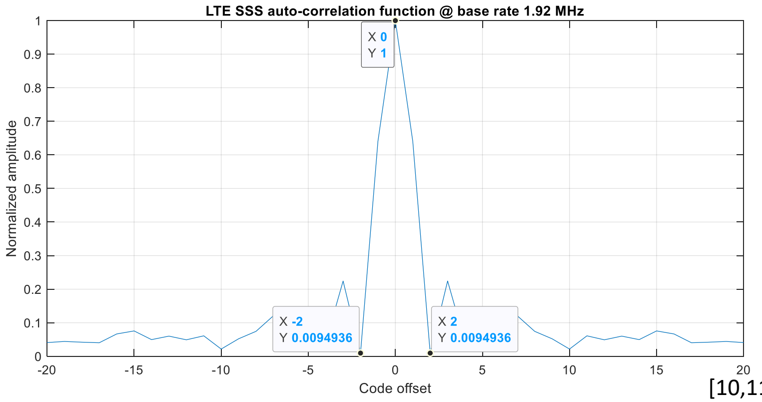

[10,11]

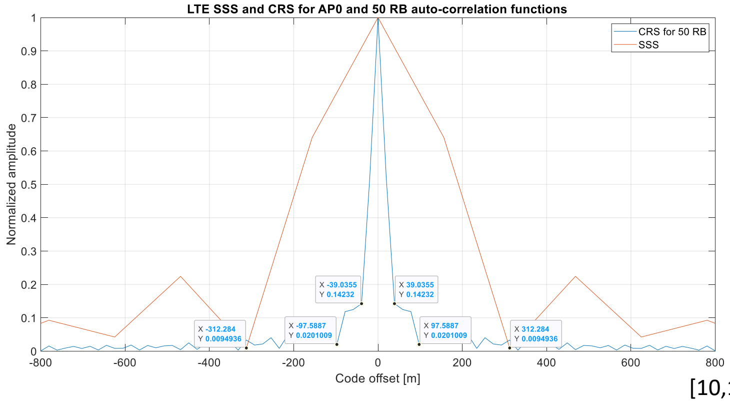

[10,11]

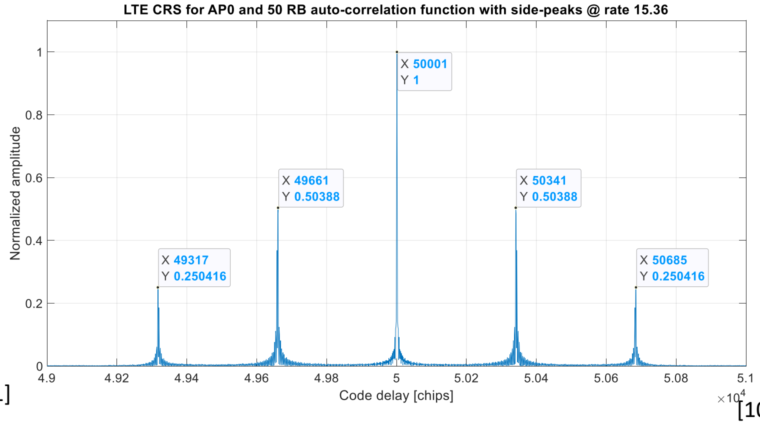

[10,11]

LTE transmitter localization - Context

- Simultaneous Localization And Mapping (SLAM) using cellular signals as Signal Of Opportunity (SoP).
- Use of carrier phase of LTE has been previously investigated within:
  - **Differential navigation framework** with Base/Navigator for:
    - indoor environments [12]
    - UAV navigation [13]
  - **Absolute positioning framework** leveraging frequency stability of LTE base station clocks for UAV navigation [13]
- Experimental results published so far assume an **a-priori known transmitter position** obtained beforehand through a collaborative mapping [14] of the transmitter.
- With dynamic receivers or UAVs → estimation of transmitter states with carrier phase measurements can potentially be realized.
- The ‘knowledge’ of transmitter states can be broadcasted as part of pseudolite signals in future.

Observation Model

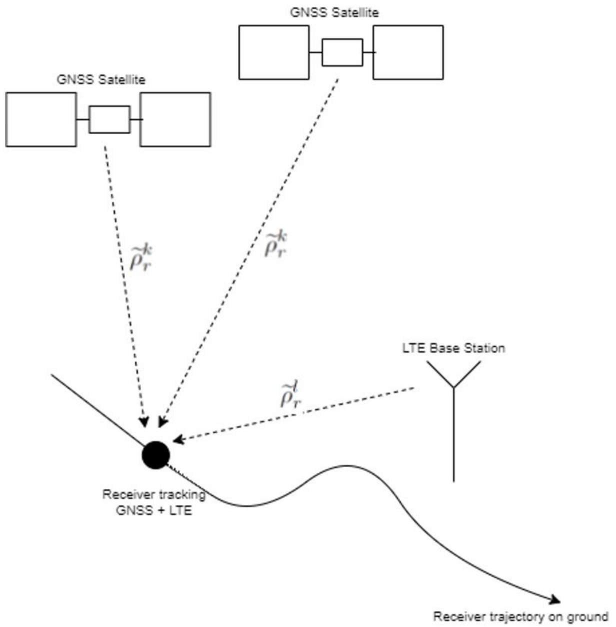

$$\begin{pmatrix}\hat{\vec{\mathbf{r}}}_l \\ \hat{\delta\tau}_l\end{pmatrix} = \arg\min_{\vec{\mathbf{r}}_l,\delta\tau_l} ||\tilde{\rho}^l_r - |\vec{\mathbf{r}}_r - \vec{\mathbf{r}}_l| - c(\delta\tau_r - \delta\tau_l)||$$

LTE TX position and clock offset

LTE pseudorange measured by receiver (MuSNAT SDR)

Known from GNSS PVT

Filter setup and simulation results

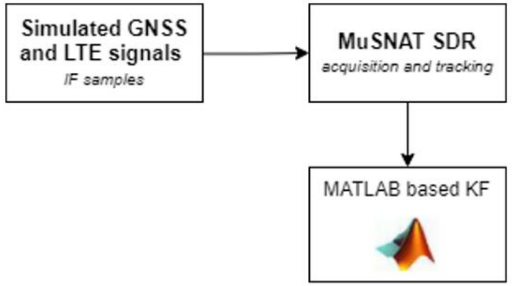

Processing chain for simulated signal

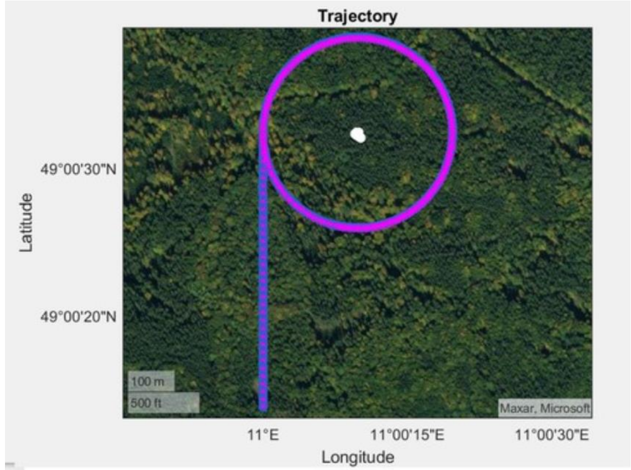

Ground track of simulated RX trajectory

Localization filter set-up → a six states Kalman Filter using code and carrier phase LTE measurements

$$\mathbf{x} = \begin{pmatrix} \vec{\mathbf{r}^l} \\ N \\ \delta\tau^l \\ \dot{\delta\tau}^l \end{pmatrix} \quad (5) \qquad \mathbf{y} = \begin{pmatrix} \rho_r^l \\ \phi_r^l \end{pmatrix}$$

$$\mathbf{B} = diag[\mathbf{I}_{4x4}, \mathbf{B}_{clk}]^{\mathrm{T}}$$

$$\mathbf{B}_{clk} = \begin{pmatrix} 1 & T \\ 0 & 1 \end{pmatrix}$$

$$\mathbf{H} = \begin{pmatrix} -(\vec{\mathbf{e}^l})^{\mathrm{T}} & 0 & -c & 0 \\ -(\vec{\mathbf{e}^l})^{\mathrm{T}} & \lambda & -c & 0 \end{pmatrix}$$

$$\mathbf{P}_0 = diag[\sigma_x^2, \sigma_y^2, \sigma_z^2, \sigma_N^2, \sigma_{\delta\tau}^2, \sigma_{\dot{\delta\tau}}^2]^{\mathrm{T}}$$

$$\mathbf{R} = diag(\sigma_\rho^2, \sigma_\phi^2)$$

$$\mathbf{Q} = diag[\Omega_x^2, \Omega_y^2, \Omega_z^2, \Omega_N^2, \mathbf{Q}_{clk}]^{\mathrm{T}}$$

$$\mathbf{Q}_{clk} = \begin{pmatrix} S_{\delta\tau_s} T + S_{\dot{\delta\tau}_s} \frac{T^3}{3} & S_{\dot{\delta\tau}_s} \frac{T^2}{2} \\ S_{\dot{\delta\tau}_s} \frac{T^2}{2} & S_{\dot{\delta\tau}_s} T \end{pmatrix}$$

Kalman Filter Time Update

$$\mathbf{x}_i^- = \mathbf{B}\mathbf{x}_{i-1}$$

$$\mathbf{P}_i^- = \mathbf{B}\mathbf{P}_{i-1}\mathbf{B}^{\mathrm{T}} + \mathbf{Q}$$

Kalman Filter Measurement Update

$$\mathbf{z}_i = \mathbf{y}_i - \mathbf{H}\mathbf{x}_i^-$$

$$\mathbf{K}_i = \mathbf{P}_i^- \mathbf{H}^{\mathrm{T}} \left(\mathbf{H}\mathbf{P}_i^- \mathbf{H}^{\mathrm{T}} + \mathbf{R}\right)^{-1}$$

$$\mathbf{x}_i^+ = \mathbf{x}_i^- + \mathbf{K}_i \mathbf{z}_i$$

$$\mathbf{P}_i^+ = (\mathbf{I} - \mathbf{K}_i\mathbf{H})\,\mathbf{P}_i^-$$

Localization Filter Results

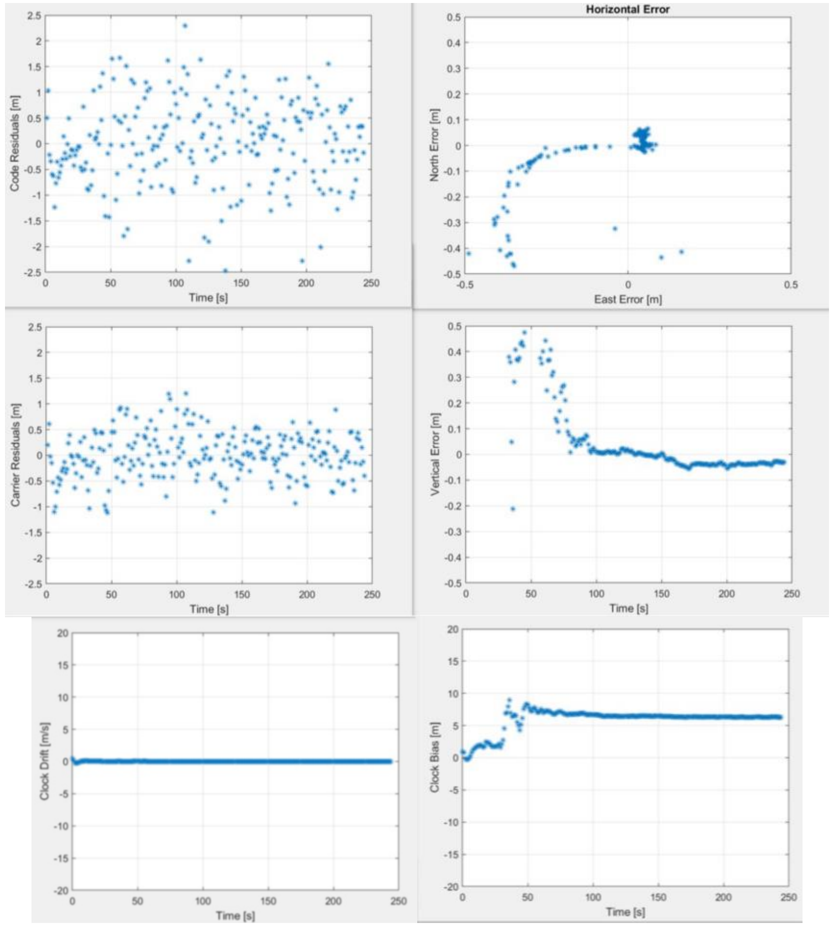

KF_states = [PosX, PosY, PosZ, floatAmbi, clkBias, clkDrift]

Estimation of carrier phase float ambiguity allows to use carrier phase for LTE transmitter localization

Experimental set-up for real-signals

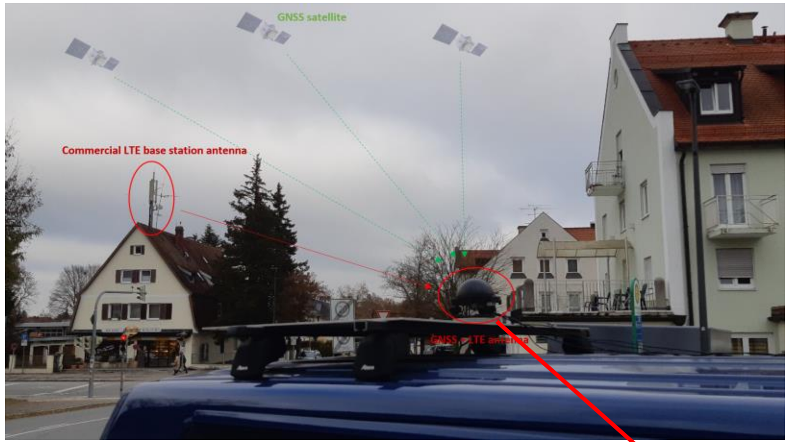

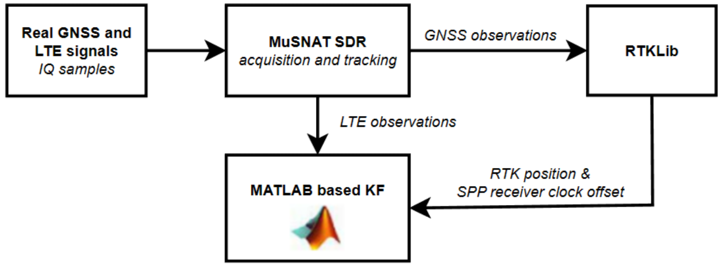

Processing chain for real signal

UAV - DJI Matrice 600 Pro drone

Ground vehicle – VW Transporter Measurement Bus

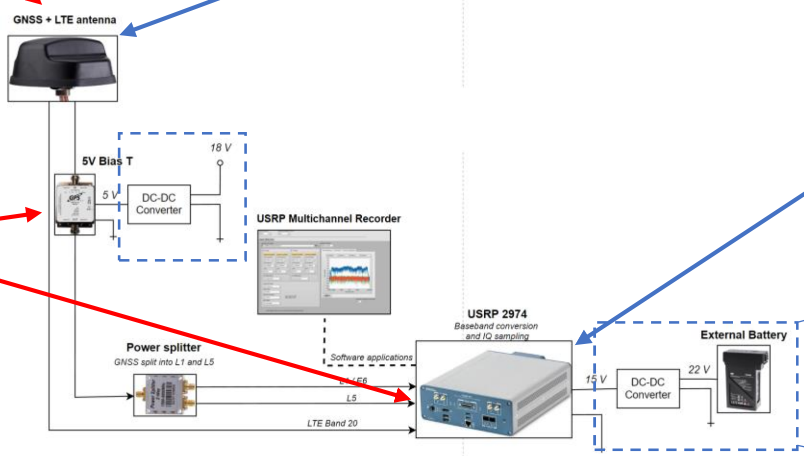

Hardware set-up

State	I_L (A)	V_o (V)	P_L (W)
USRP OFF	0.06	14.98	0.94
USRP Stand-by	2.50	14.88	37.20
USRP ON Start-up	3.50	14.86	52.01
USRP Recording 3 streams @ 20 MHz	5.00	14.74	73.70
USRP Recording 4 streams @ 20 MHz	5.20	14.73	76.60
USRP Recording 4 streams @ 40 MHz	5.50	14.71	80.91
USRP Recording 4 streams @ 50 MHz	5.78	14.70	84.97

USRP 2974 tests with external battery

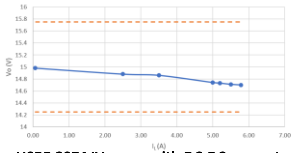

USRP 2974 IV-curve with DC-DC converter

Target base station – Amarisoft BS

Top-view of ISTA building

Amarisoft LTE TX antenna

Amarisoft BS

Research oriented BS operated by institute ETTI within UniBW M campus
- PCI 1 at f_c = 2.665 GHz
- Omni-directional antenna
- No inter-PCI clock bias or MIMO effects

Ground-truth coordinate of Amarisoft BS TX antenna measured for reference using:

- Trimble R10 used for positioning of 02 static points
- Leica MS60 used for triangulation of antenna coordinates

* PosDiff w.r.t Google Maps coordinate: [-29.71, -6.11, -33.78] m

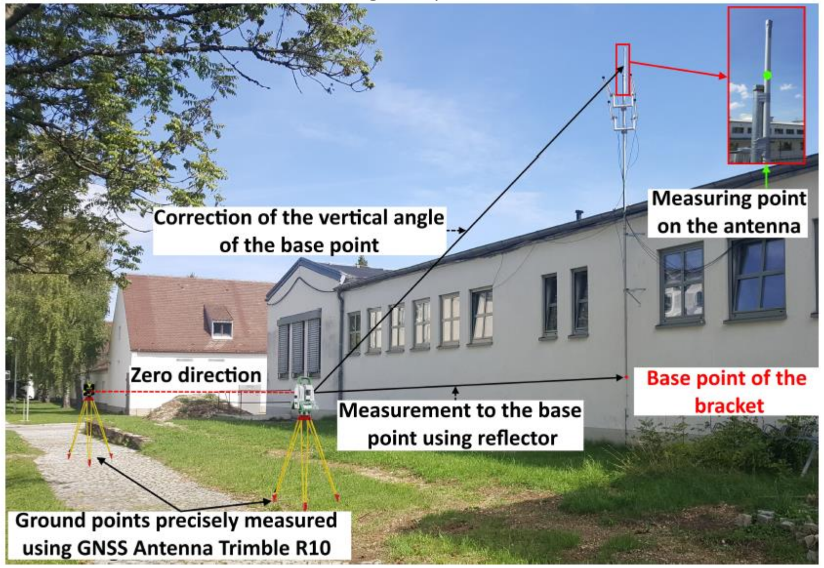

Measurement of ground-truth coordinate for Amarisoft BS

Ground vehicle with code-only measurements

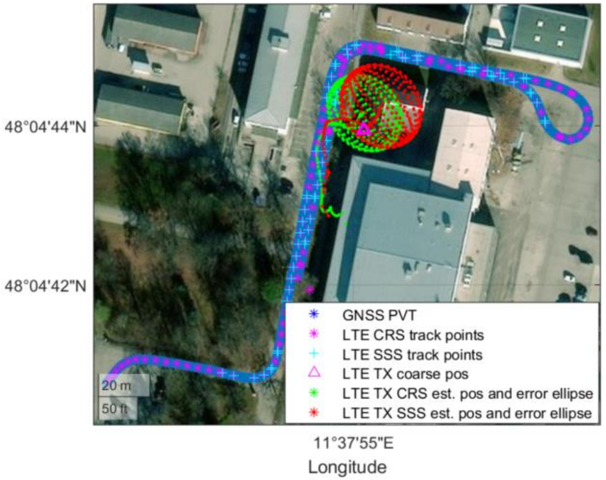

Ground vehicle trajectory

Localization filter results

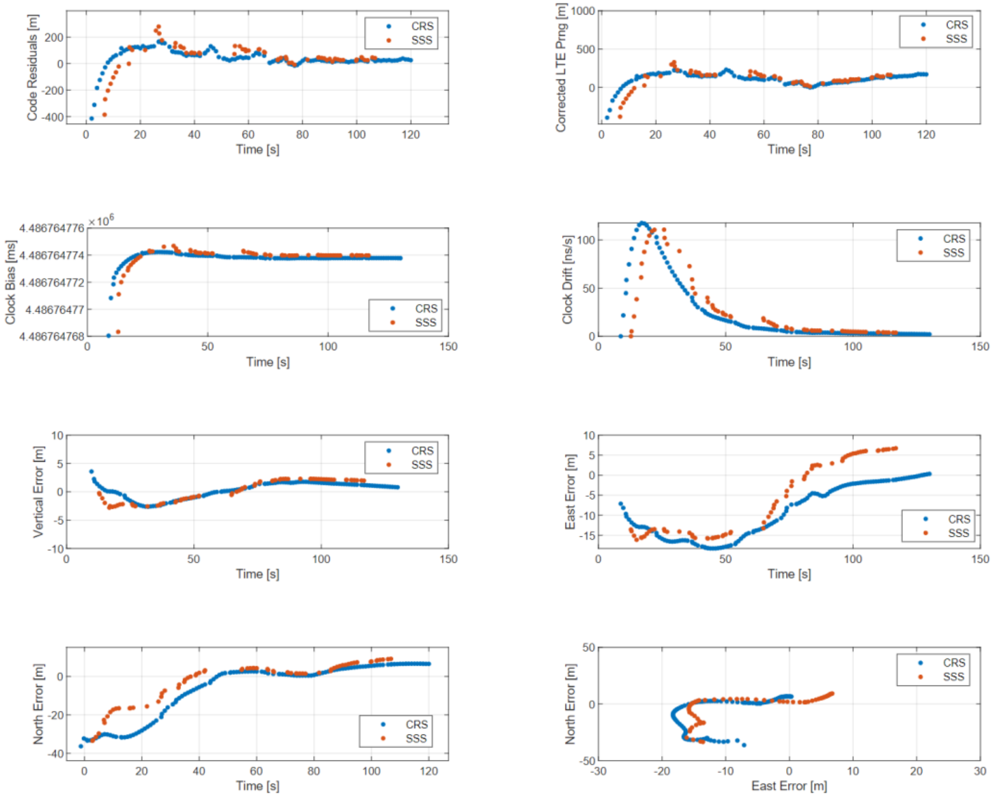

CMC Time series

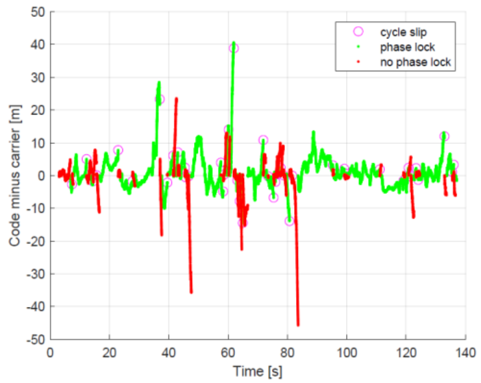

(a) Amarisoft BS CRS tracking using Measurement Bus

CMC plot indicates several cycle-slips for Ground Vehicle

Localization results using code-only measurements

State-variable	Symbol	Amarisoft BS	
		SSS	CRS
Pos. diff. X [m]*	δx	6.758	4.324
Pos. diff. Y [m]*	δy	−5.489	0.5632
Pos. diff. Z [m]*	δz	−7.606	−4.982
Absolute pos. diff.[m]*	Δ	11.56	6.621
Clock Bias [ms]	$\delta\tau$	4.49e6	4.49e6
Clock Drift [ns/s]	$\delta\dot{\tau}$	3.736	2.089

* Pos differences with respect to Google Map coordinates

CRS results are better than SSS results due to more stable signal tracking

UAV with code and carrier phase measurements

- For code + carrier measurements, 03 flights of UAV conducted near Amarisoft BS to sweep as much arc around the BS antenna as possible:

UAV flying near Amarisoft BS - photo

UAV flying near Amarisoft BS - video

Tracking results of UAV Flight 3

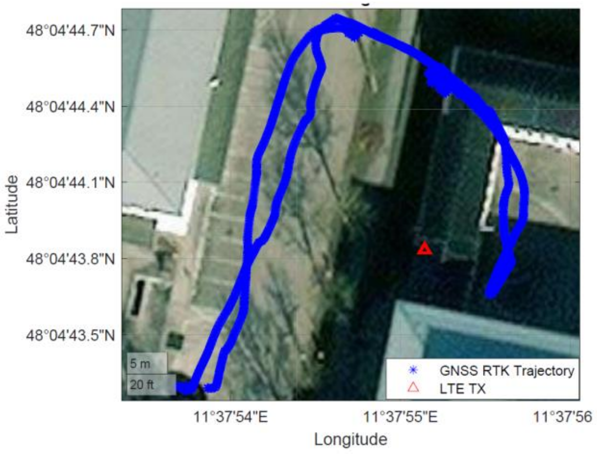

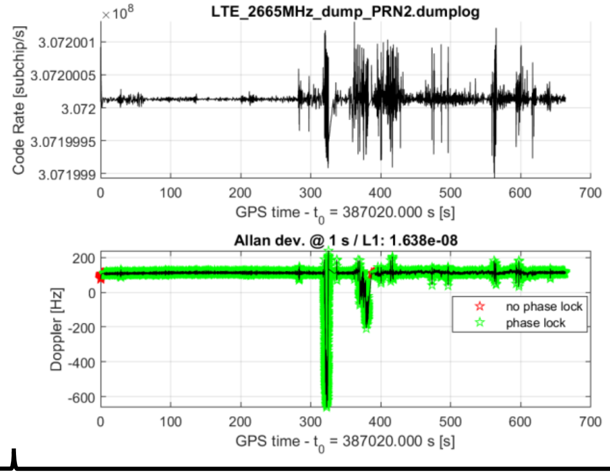

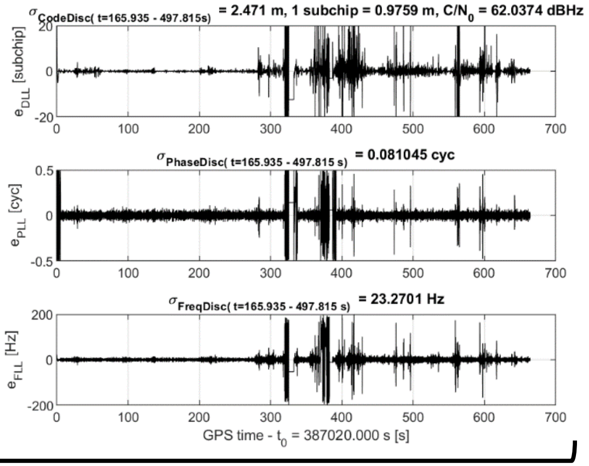

UAV flight trajectory

MuSNAT Tracking Results

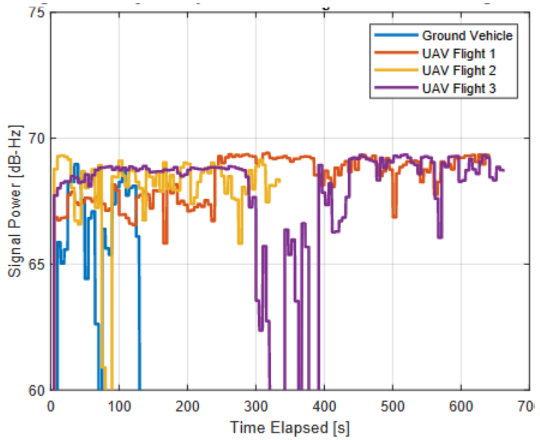

Received signal power of all measurements

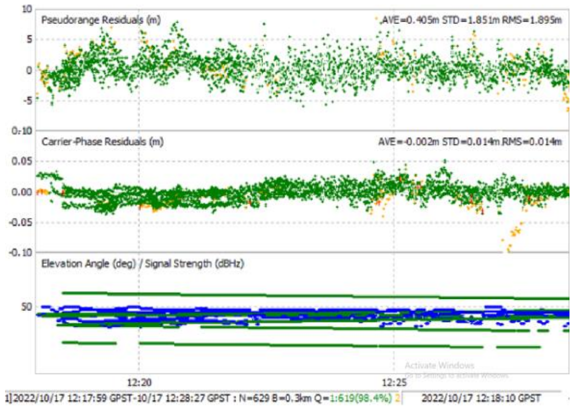

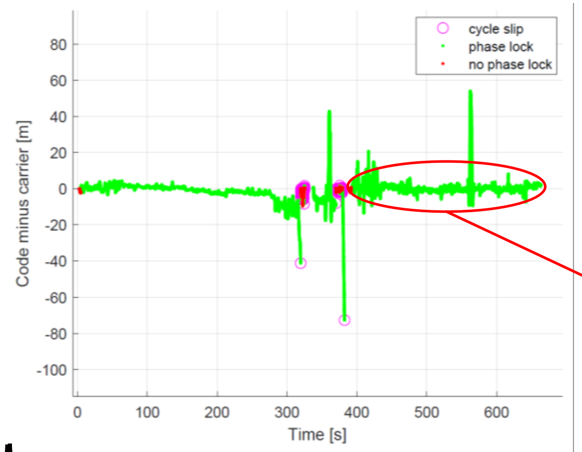

Cycle-slip free pass with low CMC and dynamic receiver ⟶ chosen for further analysis with code + carrier phase measurements

GNSS RTK results

Code-minus-carrier

Localization results of UAV Flight 3 with code and carrier phase measurements

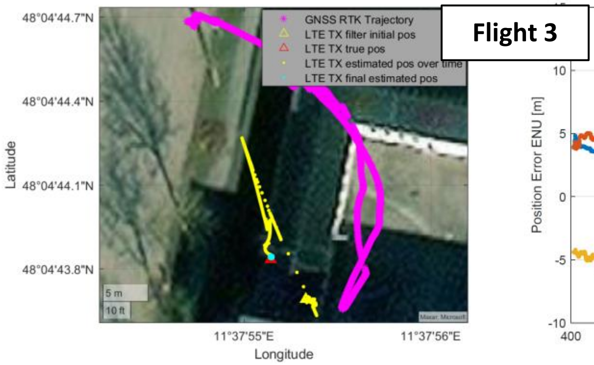

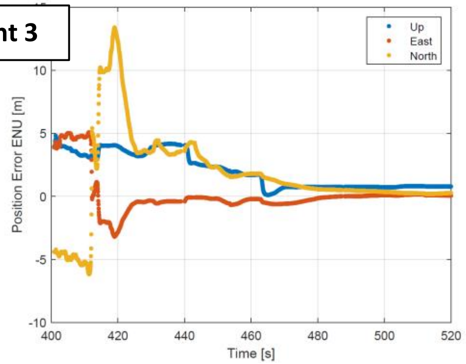

Testcase	δx [m]	δy [m]	δz [m]	norm[δx, δy, δz] [m]
Ground Vehicle	0.464	0.010	−2.28	2.33
UAV Flight 1	0.590	0.226	−1.98	2.08
UAV Flight 2	0.686	1.29	−0.405	1.52
UAV Flight 3	−0.301	−0.117	−0.770	0.834

Localization filter results

Best results achieved with UAV Flight 3 having longest stable carrier-tracking pass duration

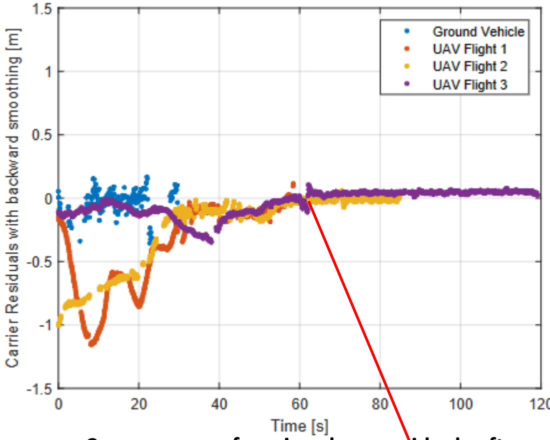

Convergence of carrier phase residuals after backward smoothing

Filter convergence time ~ 60 secs

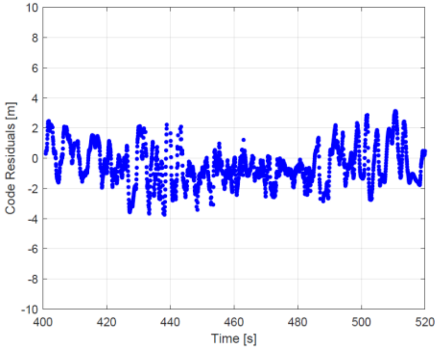

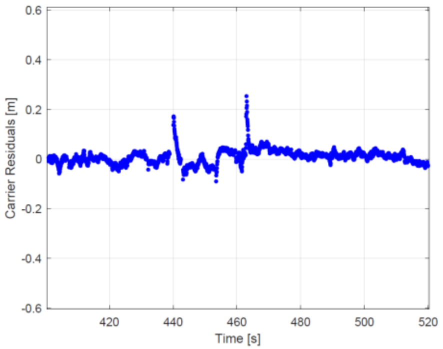

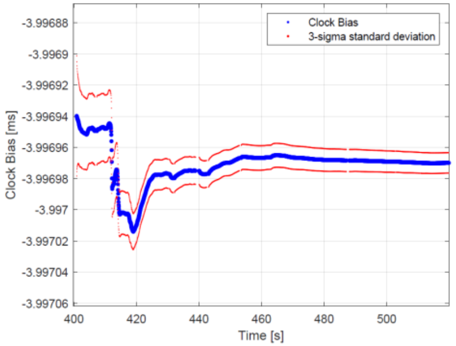

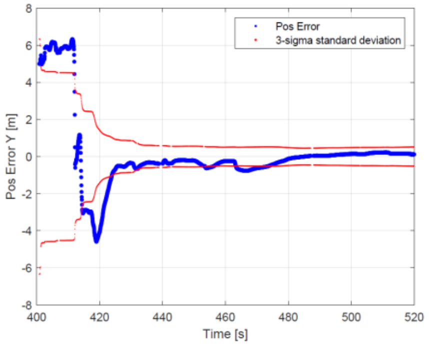

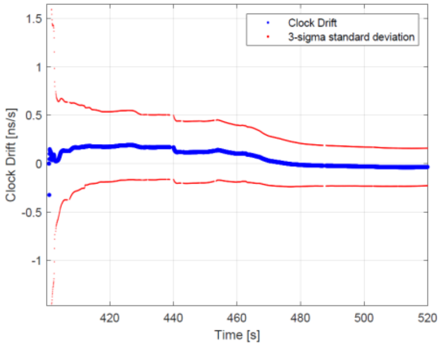

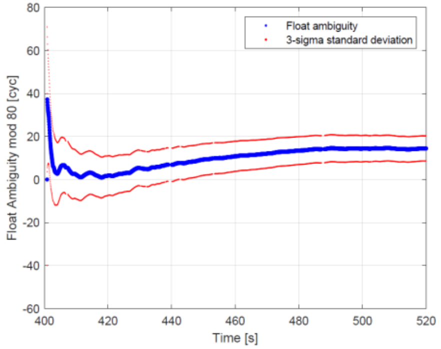

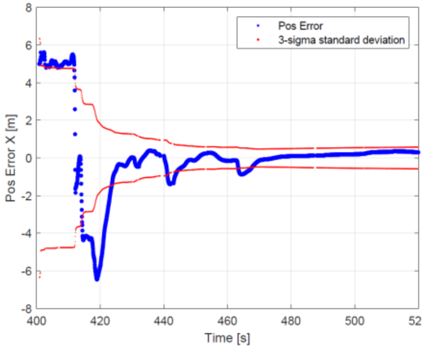

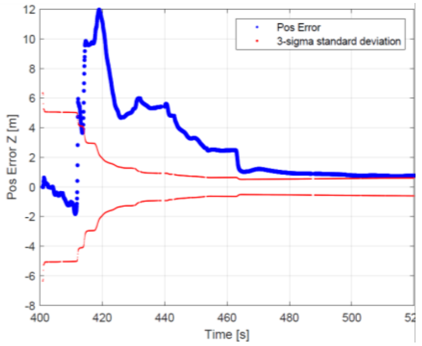

Error sources -> GNSS SPP receiver clock error

- Receiver clock offset gets eliminated in RTK
- For localization → filtered GNSS SPP clock error was used.
- 1st order polynomial fitted on measured receiver clock error
- Alternatively, a more stable on-board clock can be used.

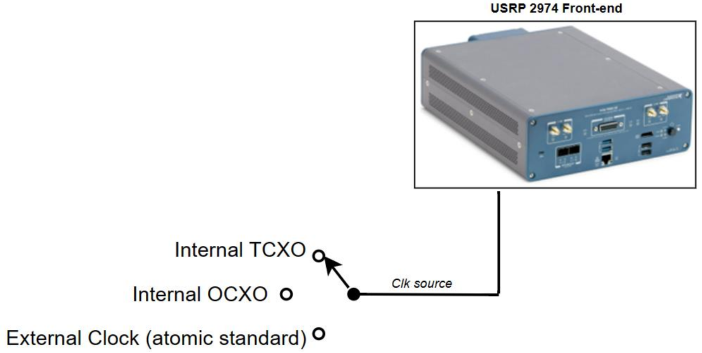

Front-end setup

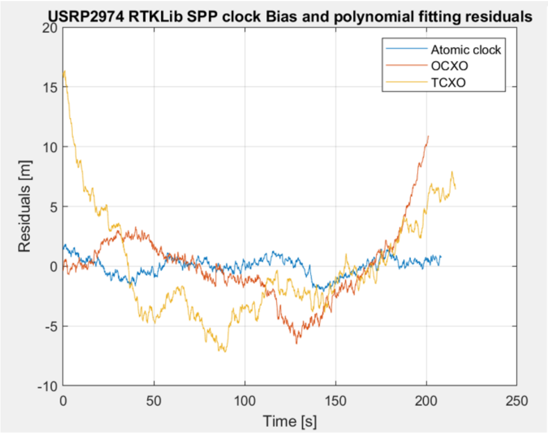

RTKLib SPP clock offset residuals w.r.t 1-order poly

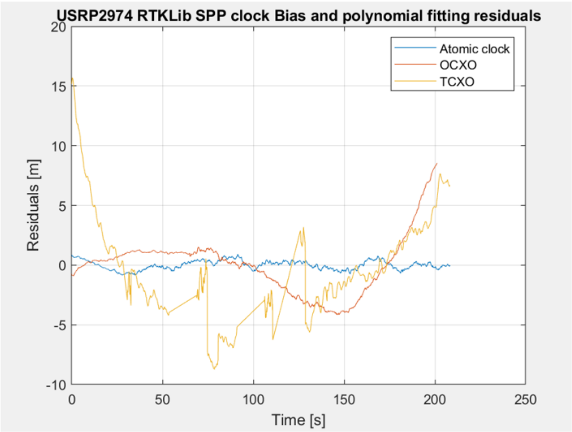

RTKLib PPP clock offset residuals w.r.t 1-order poly

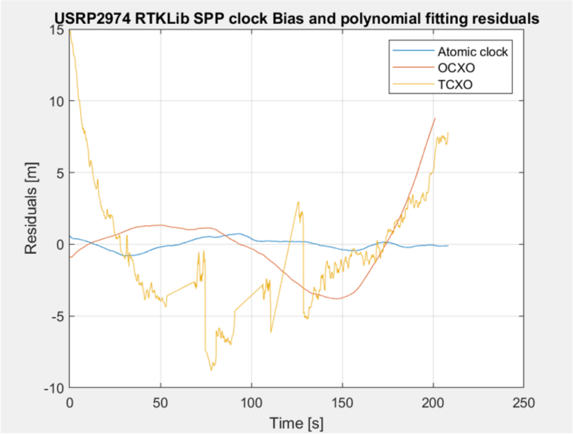

RTKLib PPP clock offset residuals (with CarriersSmoothing ON) w.r.t 1 order poly

Residuals of measured receiver clock error w.r.t 1-order polynomial for a static receiver measurement

Conclusions

- LTE signal tracking can be realized in a GNSS oriented tracking architecture.
- CRS provides a better tracking performance with high C/N_0 than SSS due to narrower correlation function and more distant Doppler side-peaks.
- Amarisoft Base station serves as a good platform for verifying calibration procedure due to easy access and availability of ground truth.
- It is possible to use carrier phase tracking of LTE signal for the purpose of transmitter localization given an accurate information of the receiver states
- Efficient cycle-slip detection scheme should be employed.
- With combined code and carrier-phase observations, a position accuracy of within 0.3 m is achieved in North and Up directions and within 1 m in the Up direction for at least one UAV flight.
- One of the biggest error sources is the SPP receiver clock offset.

Way forward

Transmitter setup

02 LTE transmitters:
Each with a different PCI
and line-of-sight position

Receiver setup

03 receivers:
- Static (base)
- Ground Vehicle (rover)
- UAV with on-board atomic clock (rover)

Testcases planned for future:

- Computation of LTE DD observations using two LTE transmitters and two receivers
- Evaluation of code and carrier phase noise of LTE CRS as function of carrier-to-noise ratio
- Comparison of code and carrier phase noise for Ground Vehicle and UAV receiver platforms
- Localization of LTE transmitter through a UAV receiver platform with on-board atomic clock
- Precise localization of LTE transmitter using LTE DD observations
- Differential positioning of a Ground Vehicle with GNSS and one LTE signal using a-priori known LTE transmitter position

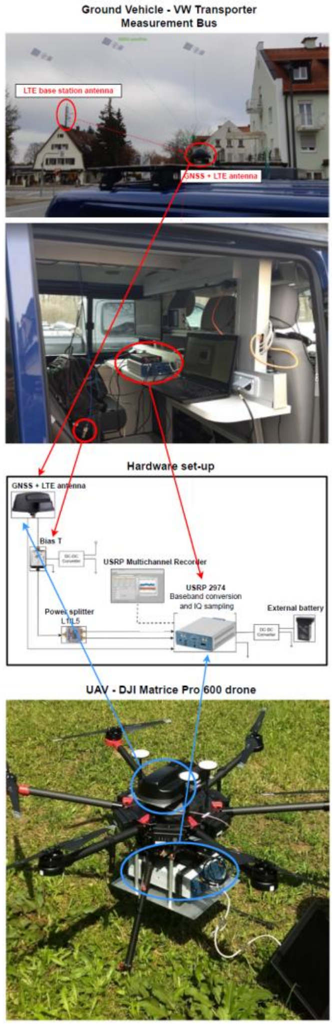

03 receivers -> Ground Vehicle, UAV and static base

References

[1] Release 9 (3gpp.org)

[2] Knutti, Fabian, Mischa Sabathy, Marco Driusso, Heinz Mathis, and Chris Marshall. "Positioning using LTE signals." In Proceedings of Navigation Conference in Europe, pp. 1-8. 2015.

[3] Shamaei, Kimia, Joe Khalife, and Zaher M. Kassas. "Exploiting LTE signals for navigation: Theory to implementation." IEEE Transactions on Wireless Communications 17, no. 4 (2018): 2173-2189.

[4] Wang, Pai, and Y. Morton. "Performance comparison of time-of-arrival estimation techniques for LTE signals in realistic multipath propagation channels." NAVIGATION, Journal of the Institute of Navigation 67, no. 4 (2020): 691-712.

[5] Shamaei, Kimia, Joe Khalife, and Zaher M. Kassas. "Comparative results for positioning with secondary synchronization signal versus cell specific reference signal in LTE systems." In Proceedings of the 2017 International Technical Meeting of the Institute of Navigation, pp. 1256-1268. 2017.

[6] Deng, Zhongliang, Xinyu Zheng, Chongyu Zhang, Hanhua Wang, Lu Yin, and Wen Liu. "A TDOA and PDR Fusion Method for 5G Indoor Localization Based on Virtual Base Stations in Unknown Areas." IEEE Access 8 (2020): 225123-225133.

[7] S. Bartelmaos, K. Abed-Meraim, and E. Grosicki, ‘‘General selection criteria for mobile location in NLoS situations,’’ IEEE Trans. Wireless Commun., vol. 7, no. 11, pp. 4393–4403, Nov. 2008.

[8] D. Liu, K. Liu, Y. Ma, and J. Yu, ‘‘Joint TOA and DOA localization in indoor environment using virtual stations,’’ IEEE Commun. Lett., vol. 18, no. 8, pp. 1423–1426, Aug. 2014.

[9] S. Li, M. Hedley, I. B. Collings, and D. Humphrey, ‘‘TDOA-based localization for semi-static targets in NLOS environments,’’ IEEE Wireless Commun. Lett., vol. 4, no. 5, pp. 513–516, Oct. 2015.

[10] M. Hameed, M. Arizabaleta, T. Pany, LTE transmitter position estimation through combined GNSS and LTE tracking using a software receiver, NAVITEC, 2022

[11] Arizabaleta-Diez, Markel, Hameed, Muhammad Subhan, Pany, Thomas, "LTE Transmitter Location and Clock State Estimation: Simulated and Real Measurements Using the SSS and CRS Signals," Proceedings of the 35th International Technical Meeting of the Satellite Division of The Institute of Navigation (ION GNSS+ 2022), Denver, Colorado, September 2022, pp. 2444-2463.

[12] Abdallah, Ali A., Shamaei, Kimia, Kassas, Zak M., "Indoor Positioning Based on LTE Carrier Phase Measurements and an Inertial Measurement Unit," Proceedings of the 31st International Technical Meeting of the Satellite Division of The Institute of Navigation (ION GNSS+ 2018), Miami, Florida, September 2018, pp. 3374-3384.

[13] J. Khalife and Z. M. Kassas, "Precise UAV navigation with cellular carrier phase measurements," 2018 IEEE/ION Position, Location and Navigation Symposium (PLANS), Monterey, CA, USA, 2018, pp. 978-989, doi: 10.1109/PLANS.2018.8373476.

[14] Morales, Joshua J., and Zaher M. Kassas. "Optimal receiver placement for collaborative mapping of signals of opportunity." In Proceedings of the 28th International Technical Meeting of the Satellite Division of The Institute of Navigation (ION GNSS+ 2015), pp. 2362-2368. 2015.

RC SPACE Research Center Space Universität der Bundeswehr München

Contact:

Muhammad S. Hameed, M.Sc.

Institute of Space Technology and Space Applications

Universität der Bundeswehr München

Email: muhammad.hameed@unibw.de

Phone: +49 (0)89 6004 4156